

An Investigation on Wear Mechanism of POM/LLDPE Blends

Jinyao Chen, Ya Cao, Huilin Li

State Key Laboratory of Polymer Materials Engineering, Polymer Research Institute of Sichuan University, Chengdu, Sichuan 610065, People's Republic of China

Received 27 December 2004; accepted 18 July 2005

DOI 10.1002/app.23626

Published online 23 March 2006 in Wiley InterScience (www.interscience.wiley.com).

ABSTRACT: The friction and wear properties of polyoxymethylene/linear low-density polyethylene/ethylene-acrylic acid (POM/LLDPE/EAA) blends are investigated on a MM-200 wear tester. The results show that the addition of LLDPE and EAA obviously improves the friction and wear properties of POM. The friction coefficient and wear scar width of POM/LLDPE/EAA blends are much lower than those of pure POM. SEM analysis reveals that POM appears to wear by thermal softening and melting of worn surface when sliding against the stainless steel, while no severe damage but wear debris can be observed on the worn face of POM/LLDPE/EAA blend. Long-time sliding causes the removal of molten POM from the worn surface, while the formation

of the lubricated layer occurs on the worn surface for POM/LLDPE/EAA blend. DSC analysis shows that the melting temperature and the crystallinity of the worn surface for POM are improved after a long-time sliding. Molecular orientation on the worn surface of POM is affirmed by WAXD. For POM/LLDPE/EAA blend, the improvement of the friction and wear properties is mainly owed to wear debris and lubricant layer existing between the contact surfaces. © 2006 Wiley Periodicals, Inc. *J Appl Polym Sci* 101: 48–53, 2006

Key words: polyoxymethylene; polyethylene (PE); friction; wear

INTRODUCTION

As an engineering plastic, polyoxymethylene (POM) resins possess strength and rigidity approaching those of nonferrous metals.^{1,2} They are hard, strong, and highly crystalline thermoplastic with a unique balance of mechanical, thermal, chemical, and electrical properties. POM resins exhibit good self-lubricant property and wear resistance.^{3–5} Consequently, they are widely applied as the rotation materials of mechanical and electromechanical fabricates electronic parts, automotives, precision instruments, etc.

Good friction and wear behaviors alone do not determine the suitability of polymers for sliding application, and the optimal conditions under which they operate must also be determined.⁶ There have been numerous investigations exploring the influence of test conditions, contact geometry, and environment on the friction and wear behavior of polymers.^{7–13} The relationship between the wear rate and the counter-face roughness for POM is more complex than that of friction. The wear of POM and POM/PTFE blends rises rapidly with the increase in roughness of the counter-face, while the wear of glass-filled POM and

carbon-filled POM is virtually insensitive to roughness over a wide range.⁶ The reduction in wear rate that may occur after polymer sliding against the steel for a certain period of time has been attributed to the transfer of the polymer onto the counter-face and the subsequent deformation of a transfer film during the initial transient period.^{14–16} In some cases, the formation of a transfer layer to the counter-surface can lead to the improvement of friction and wear properties.¹⁵ The mechanism of transfer film formation, however, is not completely understood. Transfer of materials can be promoted by an improved adhesion of polymer to the metal counter-surface by chemical modification of the metal surface or by addition of specific metal fillers to the polymer. On the other hand, there are also indications that transfer layer is formed through mechanical interlocking of polymer material and metal asperities.^{17,18}

In addition, many efforts have been carried out to investigate the wear mechanisms of POM and its composites. Kukureka et al.¹⁹ reveals that wear of POM has been divided into two regions: mild and severe. In the mild wear region, wear appears to be at least partly attributable to the mechanical fatigue of the worn surface. In the severe wear region, the cracking and subsequent rupture of the surface layer occurs. The results of Clerico²⁰ show that the wear mechanisms of POM composites are similar to delamination wear, while pure POM appears to wear by continuous deformation favored by thermal softening or melting.

Correspondence to: Y. Cao (caoya@mail.sc.cninfo.net).

Contract grant sponsor: Hi-Tech Research and Development Program of China; contract grant number: 2002AA333070.

These efforts are generally concentrated on the morphological analysis of the worn surface. Little work has been concerned with the structure change of the worn surface during sliding, which has a significant influence on the friction and wear behaviors of POM and its composites.

Our previous studies showed that the friction and wear properties of POM could be efficiently improved after adding appropriate amount of linear low-density polyethylene (LLDPE) and ethylene-acrylic acid (EAA) into POM. It is well-known that the friction and wear properties of LLDPE are poor. How can the addition of LLDPE improve the friction and wear properties of POM? To obtain a better insight in the wear mechanism of POM and POM/LLDPE/EAA blends, this study investigates the morphology and structure change of the worn surface on the basis of previous works. Moreover, the effect of the structure change of the worn surface on the friction and wear behaviors of POM and its blends are investigated.

EXPERIMENTAL

Materials

Chemically pure polyoxymethylene copolymer granular (designated as M90; melt flow rate = 9.0 g/min; specific gravity = 1.41 g/cm³) was provided by Yunnan Yuntianhua (Shuifu, Yunnan), China. LLDPE characterized by a melt index of 5.4 g/10 min (190°C, 2.16 Kg) was kindly donated by Qilu Petrochemical (Zibo, Shandong), China. EAA (Primoacor 1410) characterized by a melt rate of 1.5 g/10 min (190°C, 2.16 Kg) was supplied by Dow Plastic (Texas, USA).

Sample preparation

The mixtures of POM, LLDPE, and EAA with various weight fractions were extruded on a twin-screw extruder ($D = 15$ mm, $L/D = 22$, Nanjing, China). POM was dried in an air oven for 2 h at 80°C to remove water before extrusion. The various heating zones of the extruder were set at 170, 178, 178, and 175°C. The blank POM was also processed under the same extrusion conditions to give a thermal history similar to that of the blends.

The extrudates were palletized and then dried at 80°C for 2 h. Then the test pieces were obtained by injection molding under the following temperatures: 193, 195, 195, and 180°C. The standard pieces were prepared for further tests and characterizations.

Friction and wear testing

The friction and wear tests were conducted on an MM-200 friction and wear tester (Shanghai, China) at room temperature, according to GB3960–83. The schematic diagram of wear tester is shown in Figure 1. The

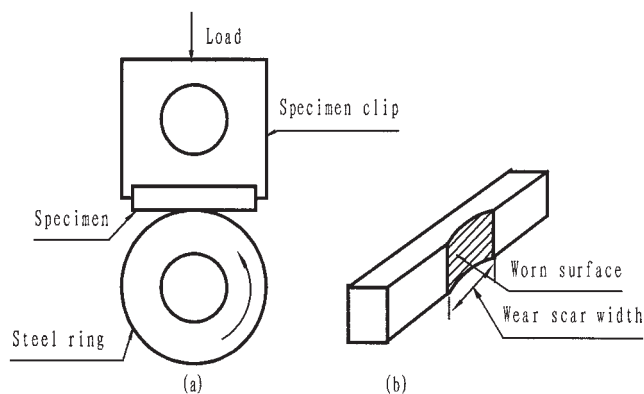


Figure 1 Schematic diagram of wear testing. (a) Scheme of MM-200 wear tester. (b) Worn surface of specimen.

dimension of the specimen is 30 × 6 × 7 mm. The rotation speed of the steel ring is 200 and 400 rpm during operation. Friction torques (T) was recorded every 5 min, and the friction coefficient was calculated as follows:

$$\mu_{\alpha} = \frac{T_{\alpha}}{MR} \quad (1)$$

where μ_{α} is the average friction coefficient, T_{α} is the average friction torque (Kg cm⁻¹), M is the load (Kg), and R is the radius of the steel ring (cm).

The wear scar widths of specimens were adopted to evaluate antiwear properties. Three replicate tests were carried out for each specimen. Before and after each test, both steel and polymer specimens were cleaned with acetone and dried.

Morphology observation

The worn surface morphology of specimens for POM and POM/LLDPE/EAA blends was observed using scanning electron microscope (JSM-5900LV, Japan).

Thermal analysis

The thermal analysis of the specimens was carried out using a Netzsch DSC 204 (Netzsch, Germany) differential scanning calorimeter. The samples were first rapidly heated up to 200°C and maintained at this temperature for 5 min to erase any previous thermal history. Then the sample was cooled down to room temperature at a cooling rate of 10°C/min. It was subsequently heated up to 200°C at a heating rate of 10°C/min to determine crystal melting information.

X-ray diffraction

WAXD were taken on a Philip X'pert prd diffractometer (Japan) with Ni-filtered Cu α radiation at room temperature. Accelerating voltage and electron cur-

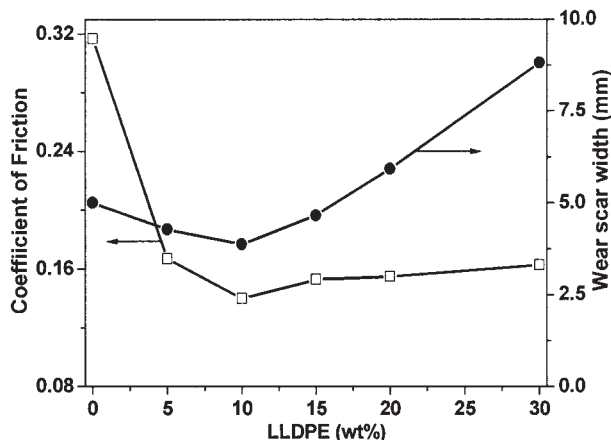


Figure 2 Variation of friction and wear properties with LLDPE content in POM/LLDPE/EAA blends (EAA, 4 wt % speed, 200 rpm; load, 30 Kg; time, 30 min).

rent were 40 kV and 40 mA, respectively. The scanning angle ranged from 15° to 60° (2θ).

RESULTS AND DISCUSSION

Friction and wear behaviors of POM/LLDPE/EAA blends

The friction and wear properties of POM/LLDPE/EAA blends are shown in Figure 2. The friction coefficient of POM/LLDPE/EAA blends decreases remarkably with LLDPE contents when the EAA content is 4 wt %. The wear scar width of POM/LLDPE/EAA blends also declines with the LLDPE content until the LLDPE content is less than 10 wt %. When the LLDPE content is over 10 wt %, the wear scar width of POM/LLDPE/EAA blends goes up. POM/LLDPE/EAA (86/10/4) blend shows approximately a 56% decrease in the friction coefficient compared to POM, and the wear scar width decreases 24.4% from 5.00 (POM) to 3.88 mm. This result indicates that the fric-

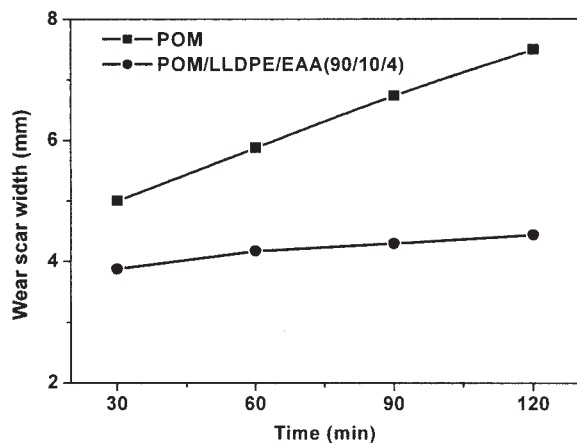


Figure 3 Variation of wear scar width of specimens with time (speed, 200 rpm; load, 30 Kg).

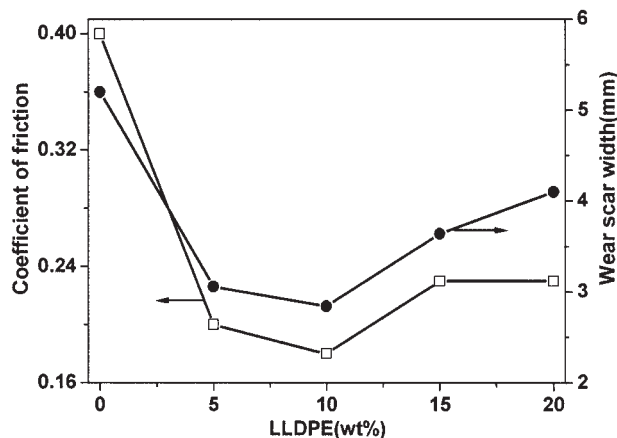


Figure 4 Variation of friction and wear properties with LLDPE contents in POM/LLDPE/EAA blends (EAA, 4% speed, 400 rpm; load, 10 Kg; time, 20 min).

tion and wear properties of POM get effectively improved after the addition of LLDPE and EAA.

It can be observed from Figure 3 that the wear scar width of POM and POM/LLDPE/EAA (86/10/4) blend increases with sliding time. The wear scar width of POM is above 49% from 5.00 mm (30 min) to 7.46 mm (120 min), while the wear scar width of POM/LLDPE/EAA (86/10/4) blend increases only by 14% from 3.88 mm (30 min) to 4.44 mm (120 min) under the same condition. This means the wear of POM is much more sensitive to time than that of POM/LLDPE/EAA (86/10/4) blend. The wear scar width of POM is much greater than that of its blend in the whole experimental time, which indicates that antiwear property of POM/LLDPE/EAA blends in the long time get has greatly improved.

At the high-speed condition (400 rpm), the friction and wear properties of POM/LLDPE/EAA blends are shown in Figure 4. The friction and wear behaviors of POM/LLDPE/EAA blend at high speed are similar to those at low speed. The friction coefficient and wear scar width of POM also decrease remarkably after the addition of LLDPE and EAA.

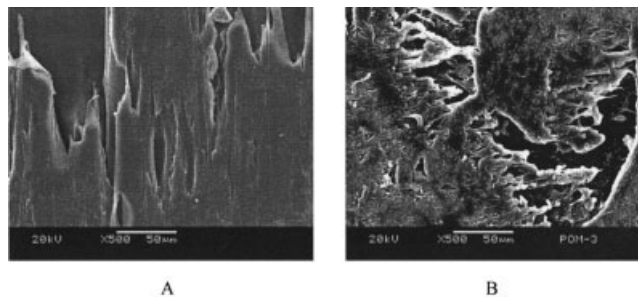


Figure 5 SEM of the worn surface of POM. (A) Speed, 200 rpm; load, 30 Kg; time, 120 min. (B) Speed, 400 rpm; load, 10 Kg; time, 30 min.

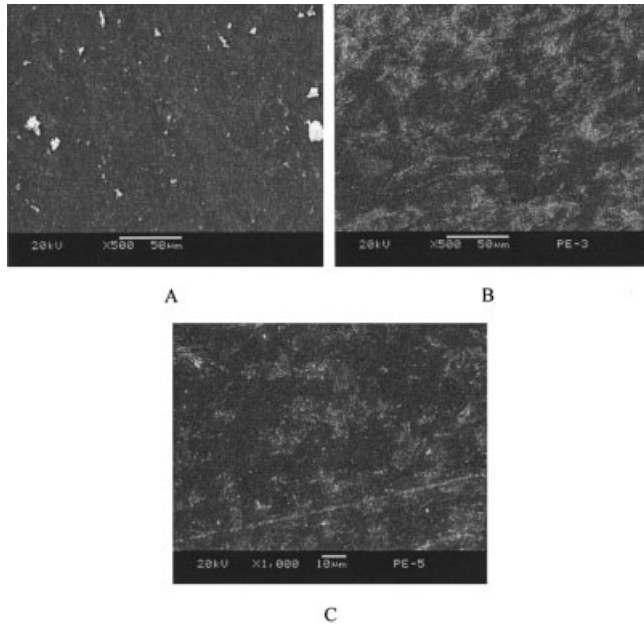


Figure 6 SEM of the worn surface of POM/LLDPE/EAA (86/10/4) blend. (A) Speed, 200 rpm; load, 30 Kg; time, 120 min. (B) Speed, 200 rpm; load, 30 Kg; time, 180 min. (C) Speed, 400 rpm; load, 20 Kg; time, 30 min.

Wear mechanisms of POM and POM/LLDPE/EAA blends

The scanning electron micrographs of the worn surface for POM and POM/LLDPE/EAA blend under various conditions are shown in Figure 5. After POM sliding against the steel counterface for 120 min, the repeated sliding causes the thermal softening and melting of the surface layer materials [Fig. 5(A)]. The wear of POM aggravates due to thermal softening or melting of the worn surface, which indicates that the wear mechanism of POM is similar to typical adhesion wear.

Figure 5(B) exhibits the SEM image of the worn surface of POM at high speed (400 rpm). The removal of molted POM from the matrix and thermal destruc-

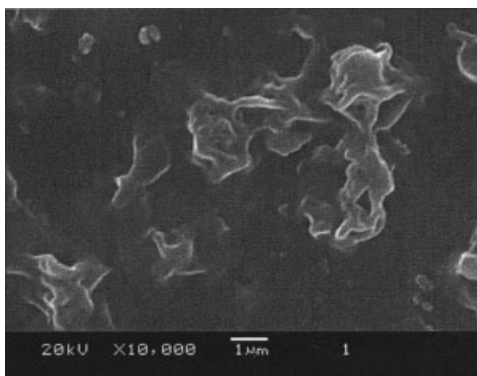


Figure 7 SEM micrograph of POM/LLDPE/EAA (86/10/4) blend wear debris produced during sliding (speed, 200 rpm; load, 30 Kg; time, 120 min).

TABLE I
DSC Thermogram Data of POM

Specimen	T_{onset} (°C)	T_{peak} (°C)	X_c (%)
POM			
Bulk	137.2	143.1	69.4
Surface	138.3	146.4	82.4
Debris	139.7	148.3	82.9

tion of polymer takes place. It can be deduced that the friction-induced temperature rise of the worn surface has reached or exceeded the thermal resistance of POM at high sliding speed. The wear of POM becomes more serious due to the thermal softening and melting of the worn surface.

The worn surface morphologies of POM/LLDPE/EAA blend under different conditions are given in Figure 6. Compared to POM, no serious damage but wear debris is observed on the worn surface of POM/LLDPE/EAA blend [Fig. 6(A)]. Wear debris existing between the steel ring and POM matrix acts as rolling lubricants, which helps to improve the friction and wear properties of POM/LLDPE/EAA blend. At low speed and long-period sliding or at high speed, the morphologies of POM/LLDPE/EAA blend are similar [Fig. 6(B) and (C)]. The lubricant layer formed on the worn surface of POM/LLDPE/EAA blend may be due to the melting of wear debris, which results from the long time shearing, stretching, and the friction-induced temperature rising during sliding. The lubricant layer between the contact surfaces reduces the friction and wear properties of POM to a much lower level.

The above results indicate that wear debris play an important role in improving the friction and wear behaviors of POM/LLDPE/EAA blend. Therefore, a general survey is carried out on the collected wear debris on the steel ring surface. At high magnifications, it can be clearly seen from Figure 7 that wear debris exhibit lamellar structure, and most of them possess uneven edges and molten surfaces, indicative of plastically stretching and melting. This affirmed that the formation of lubricant layer on the worn surface of POM/LLDPE/EAA blend is just due to the molten of the wear debris.

TABLE II
DSC Thermogram Data of POM/LLDPE/EAA (86/10/4) Blend

Specimen	T_{onset} (°C)	T_{peak} (°C)	X_c (%)
POM/LLDPE/EAA (86/10/4) ^a			
Bulk-POM	143.1	145.3	51.0
Surface-POM	143.2	145.7	56.4
Bulk-LLDPE	104.2	106.4	27.5
Surface-LLDPE	103.9	106.4	26.1

^a 200 rpm, 30 kg, 120 min.

TABLE III
Calculated Results of WAXD on the Worn Surface of POM

Wear time	Unit cell parameter		Crystalline size, D (nm)			Crystalline degree, X_c (%)
	$a = b$ (nm)	c (nm)	L_{100}	L_{105}	L_{110}	
0 min	0.448	1.738	17.003	10.337	19.679	73.4
120 min	0.448	1.756	14.687	10.751	11.950	86.2

To obtain a better insight in the wear mechanism, the structure and morphology of worn surface for POM and POM/LLDPE/EAA blend was investigated. DSC data of the bulk, the worn surface, and the wear debris of POM after sliding 120 min against the steel counterface are listed in Table I. For POM, the onset and peak melting temperatures of the worn surface, which are 138.3 and 146.4°C, respectively, raise 1.1 and 3.3°C over those of POM bulk. The onset and peak melting temperatures of the wear debris, which are 139.7 and 148.3°C, respectively, are much higher than those of the bulk. In addition, the crystallinity also rises from 69.4% of the bulk to 82.4% of the worn surface and 82.9% of the wear debris. The increase of the melting temperature and the crystallinity of the worn surface indicate that the friction-induced temperature rise of the worn surface during sliding is high enough to cause POM to be annealed, which makes the crystal morphology more perfect and the crystallinity higher.

For POM/LLDPE/EAA blend, the changes of crystal melting temperature and crystallinity of the bulk and the worn surface for POM and LLDPE in the blend are not so apparent, as shown in Table II. These results indicate that the structure and morphology of the worn surface for POM/LLDPE/EAA blend are different to that of POM. The annealing effect of POM/LLDPE/EAA blend is not as adequate as that of POM during sliding. Wear debris and the lubricant layer between the steel ring and POM/LLDPE/EAA blend help to decrease the friction coefficient and the temperature of the worn surface. Although it is too difficult to measure the surface temperature *in situ*, the surface temperature of the steel ring sliding against POM is obviously higher than that sliding against POM/LLDPE/EAA blend.

WAXD analysis data of the worn surface for POM and POM/LLDPE/EAA (86/10/4) blend under the given condition (200 rpm, 30 Kg, 120 min) are shown in Tables III and IV. The crystal structure of the worn

surface of POM does not change after POM sliding 120 min against the steel ring. The crystallinity increases from 73.4 to 86.2% and the microcrystalline size of POM decreases during sliding. It can be seen from Table IV that the changes of the crystallinity and the microcrystalline size of POM in POM/LLDPE/EAA (86/10/4) blend are not as apparent as those of POM during sliding. The results of WAXD are agreeable to those of DSC.

Relative orientation degree (Π) of polymer materials is generally calculated according to the following equation²¹:

$$\Pi = \frac{180^\circ - H}{180^\circ} \times 100\% \quad (2)$$

where H is the full width at half maximum. Relative orientation degree of $[hkl]$ in the worn surface for POM and POM/LLDPE/EAA (86/10/4) blend is listed in Table V. Compared to POM, the variation of relative orientation degree of the worn surface of POM/LLDPE/EAA blend is not noticeable after sliding for 120 min. Wear debris and the lubricant layer existing between the contact surfaces help to decrease the temperature of the worn surface and release the interaction between POM/LLDPE/EAA blend and the steel counterface, and results in the change of the surface structure of POM/LLDPE/EAA blend, which is not so apparent.

Friction and wear model of POM and POM/LLDPE/EAA blends

POM appears to wear by thermal softening and melting. When POM slides against the stainless steel ring, the friction coefficient is higher and more friction heat is produced; therefore, the temperature of worn surface will be higher with sliding time. The high temperature causes POM to be annealed, which makes crystallinity and hardness of worn surface higher. The

TABLE IV
Calculated Results of WAXD on the Worn Surface of POM/LLDPE/EAA (86/10/4) Blend

Wear time	Unit cell parameter		Crystalline size (nm)			Crystalline degree, X_c (%)
	$a = b$ (nm)	c (nm)	L_{100}	L_{105}	L_{115}	
0 min	0.442	1.745	14.386	8.542	8.498	50.3
120 min	0.448	1.746	17.134	9.560	9.132	54.4

evidence of molecular orientation on the worn surface of POM was identified by WAXD. When harder surface slides against the steel ring, the temperature of worn surface rises much higher. After a long sliding time or under high speed and high load, the temperature of worn surface will approach to or reaches softening point of POM, which causes worn surface to soften or melt. Some extrusion of molten POM from the contact region is observed on the worn surface and the transfer film is found on the steel counterface, which accelerates the wear of POM [Fig. 8(A)]. Therefore we can conclude that the wear mechanisms of POM include abrasive wear, adhesion wear, and fatigue wear.

For POM/LLDPE/EAA blends, wear debris produced during sliding exist in the contact region, which acts as rolling lubricants. Therefore, the friction coefficient is lower and less friction heat will be generated, the surface temperature of POM/LLDPE/EAA blend will be lower compared with POM. After a long sliding time or under high speed and high load, the lubricant film is formed on the worn surface because of the molten wear debris, which isolates effectively the interaction between the two contact surfaces. The friction and wear behaviors of POM/LLDPE/EAA blends get greatly improved. The structure and morphology of the worn surface of POM/LLDPE/EAA blends is different from POM. Wear debris and the lubricant layer are favorable to decrease the friction coefficient and the temperature of the worn surface. Therefore, the orientation and the crystalline degree of POM do not apparently generate changes on the worn surface of POM/LLDPE/EAA blend. This reduction of friction and wear properties by interposed wear debris and the lubricant layer may have the same

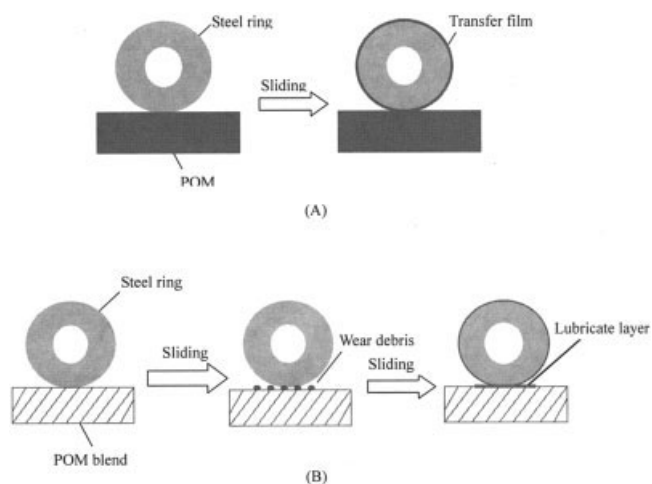


Figure 8 The diagrammatic sketches of the sliding wear model.(A) Sliding against POM. (B) Sliding against POM/LLDPE/EAA blend.

general principles as a small amount of sand and lubricant oil are present. This model is a further application of the principle that in dry sliding there should be a "third body" presented between the sliding surface to decrease friction and wear and it is summarized as in Figure 8(B).

References

- Weber, M. *Kunststoffe Plast Europe* 1998, 88, 29.
- Boehme, E. *Plastics* 1972, 25, 114.
- Masamoto, J. *J Appl Polym Sci* 1993, 50, 1299.
- Masamoto, J. *J Appl Polym Sci* 1993, 50, 1307.
- Masamoto, J. *J Appl Polym Sci* 1993, 50, 1317.
- Odi-Owei, S.; Schipper, D. J. *Wear* 1991, 148, 363.
- Unal, H.; Mimaroglu, A. *Mater Des* 2003, 24, 183.
- Tanaka, K. *Trans ASME JOT* 1977, 99, 408.
- Kar, M. K.; Bahadur, S. *Wear* 1974, 30, 337.
- Santner, E.; Czichos, H. *Tribol Int* 1989, 22, 103.
- Clerico, M. *Wear* 1969, 13, 183.
- Stuart, B. H. *Tribol Int* 1998, 31, 647.
- Yamaguchi, Y. *Tribology of Plastic Materials: Their Characteristics and Applications to Sliding Components*; Elsevier: Amsterdam, 1990.
- Ziemianski, K.; Capanidis, D. *Wear* 1982, 82, 317.
- Kar, M. K.; Bahadur, S. *Wear* 1978, 46, 189.
- Rhee, S. H.; Ludema, K. C. *Wear* 1978, 46, 231.
- Lavielle, L. *Wear* 1991, 151, 63.
- Marcus, K.; Allen, C. *Wear* 1994, 178, 17.
- Kukureka, S. N.; Chen, Y. K.; Hooke, C. J.; Liao, P. *Wear* 1995, 185, 1.
- Clerico, M. *Wear* 1980, 64, 259.
- Yin, J. H.; Mo, Z. S. *Modern Polymer Physics*; Science Press: Beijing, 2001.
- Godet, M. *Wear* 1984, 100, 437.

TABLE V
Relative Orientation Degree of $[hkl]$ in the Worn Surface in POM and POM/LLDPE/EAA (86/10/4) Blend

Wear time	Relative orientation degree			
	Π_{100}	Π_{105}	Π_{110}	Π_{115}
POM				
$\mu 0$ min	82.4	70.4	77.4	—
$\mu 120$ min	86.8	75.4	85.9	—
POM/LLDPE/EAA (86/10/4)				
$\mu 0$ min	82.0	68.9	—	67.3
$\mu 120$ min	84.5	72.3	—	69.6